Germanate with Three-Dimensional 12 × 12 × 11-Ring Channels Solved by X-ray Powder Diffraction with Charge-Flipping Algorithm

ARTICLE *in* INORGANIC CHEMISTRY · FEBRUARY 2013

Impact Factor: 4.76 · DOI: 10.1021/ic302705f · Source: PubMed

6 AUTHORS, INCLUDING:

Yan Xu
Northwestern University
15 PUBLICATIONS **46** CITATIONS
SEE PROFILE

Leifeng Liu
Stockholm University
18 PUBLICATIONS **119** CITATIONS
SEE PROFILE

Daniel M. Chevrier
Dalhousie University
20 PUBLICATIONS **251** CITATIONS
SEE PROFILE

Junliang Sun
Peking University
169 PUBLICATIONS **2,466** CITATIONS
SEE PROFILE

Inorganic Chemistry

Article

pubs.acs.org/IC

Germanate with Three-Dimensional 12 × 12 × 11-Ring Channels Solved by X-ray Powder Diffraction with Charge-Flipping Algorithm

Yan Xu,[†,#] Leifeng Liu,[‡,#] Daniel M. Chevrier,[∥] Junliang Sun,*[,‡,§] Peng Zhang,*[,∥] and Jihong Yu*[,†]

[†]State Key Laboratory of Inorganic Synthesis and Preparative Chemistry, College of Chemistry, Jilin University, Changchun 130012, China

[‡]Berzelii Center EXSELENT on Porous Materials, Department of Materials and Environmental Chemistry, Stockholm University, Stockholm SE-106 91, Sweden

[§]College of Chemistry and Molecular Engineering, Peking University, Beijing 100871, China

[∥]Department of Chemistry, Dalhousie University, 15000, Halifax, Nova Scotia, Canada NS B3H 4R2

Supporting Information

ABSTRACT: A new open-framework germanate, denoted as GeO-JU90, was prepared by the hydrothermal synthesis method using 1,5-bis(methylpyrrolidinium)pentane dihydroxide as the organic structure-directing agent (SDA). The structure of GeO-JU90 was determined from synchrotron X-ray powder diffraction (XRPD) data using the charge-flipping algorithm. It revealed a complicated framework structure containing 11 Ge atoms in the asymmetric unit. The framework is built of 7-connected Ge_7 clusters and additional tetrahedral $GeO_3(OH)$ units forming a new three-dimensional interrupted framework with interesting 12 × 12 × 11-ring intersecting channels. The Ge K-edge extended X-ray absorption fine structure (EXAFS) analysis was performed to provide the local structural information around Ge atoms, giving rise to a first-shell contribution from about 4.2(2) O atoms at the average distance of 1.750(8) Å. The guest species in the channels were subsequently determined by the simulated annealing method from XRPD data combining with other characterization techniques, e.g., ^{13}C NMR spectroscopy, infrared spectroscopy (FTIR), compositional analyses, and thermogravimetric analysis (TGA). Crystallographic data $|(C_{15}N_2H_{32})(NH_4)|[Ge_{11}O_{21.5}(OH)_4]$, orthorhombic *Ama*2 (No. 40), a = 37.82959 Å, b = 15.24373 Å, c = 12.83659 Å, and Z = 8.

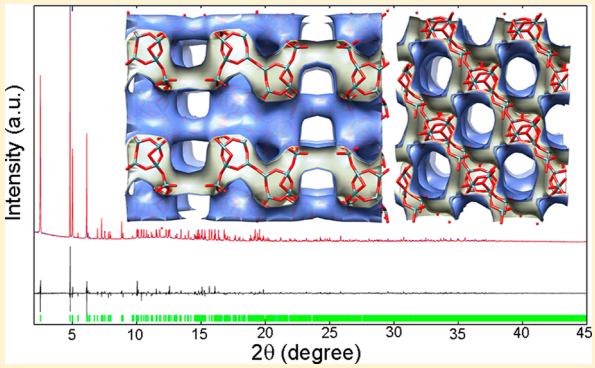

INTRODUCTION

Crystalline porous materials, especially zeolites with open-framework structures, are widely used in industry due to their excellent catalytic, ion-exchange, and adsorption properties.[1] Since these properties strongly depend on the channel system of the framework structure, much effort has been made to explore open-framework materials with novel structures in the past decades.[2] Open-framework germanates are of particular interest for their ability to form diverse structures, especially structures with an extralarge pore.[3−6] In contrast to silicate-based zeolite materials that contain only tetrahedral primary building units, open-framework germanates can be constructed from a variety of Ge-centered coordination polyhedra including Ge-centered tetrahedra, trigonal bipyramids, and octahedra. Combination of these flexible coordination modes of the Ge atom leads to formation of some well-defined clusters including Ge_7X_{19} (Ge_7),[3] Ge_8X_{20} (Ge_8),[4] Ge_9X_{25-26} (Ge_9),[3g,l,5] $Ge_{10}X_{28}$ (Ge_{10}),[6] and Ni@Ge_{14} clusters,[7] where X = O, OH, or F. These large cluster building units can then be linked to each other by sharing O atoms or through additional primary building units, for instance, GeO_4 tetrahedra to form a variety of open-framework structures with large pores, as predicted by Férey on the basis of the concept of "scale chemistry".[8] For example, ASU-16[3b] and SU-12[3f] with 24-ring channels are built of Ge_7 and $(Ge,Si)_7$ clusters, respectively; FDU-4[5d] with 24-ring channels is built of Ge_9 clusters; SU-M[6b] with mesoporous 30-ring channels is built of Ge_{10} clusters; JLG-12[3l] with mesoporous 30-ring channels is built of the combination of Ge_7 and Ge_9 clusters; FJ-1[7] with 24-ring channels is built of Ni@Ge_{14} clusters.

Among the various Ge clusters, the Ge_7 cluster has been frequently observed in the open-framework germanate compounds.[3] The Ge_7 cluster is a pseudocubic building unit ("4−3" subunit) consisting of four GeO_4 tetrahedra, two GeO_5 trigonal bipyramids, and one GeO_6 octahedron. It has a maximum connectivity of 7 but is more frequently observed to have a lower connecting number. A list of germanates with various connection modes of the Ge_7 cluster is given in Table 1. It is rare to find the fully connected Ge_7 clusters in the reported

Received: December 9, 2012

   dx.doi.org/10.1021/ic302705f | Inorg. Chem. XXXX, XXX, XXX−XXX

Table 1. Various Connection Modes of Ge_7 Clusters[a]

mode of linkage	n connection	example	dimension	ref
T^2	2	FJ-6	1D	3e
P^2O	3	unknown		
T^4	4	ASU-20-DACH	2D	3c
		ASU-20-DAPe	2D	3c
		JLG-4	1D	3k
		JLG-5	1D	3j
		JLG-12	3D	3l
T^2P^2	4	SU-44	3D	3g
		SU-MB	3D	6b
T^2PO	4	unknown		
T^4P	5	ASU-12	3D	3a
		ASU-16	3D	3b
		ASU-19	2D	3c
		SU-12	3D	3f
T^4O	5	ASU-19	2D	3c
T^4P^2	6	SU-44	3D	3g
T^4PO	6	SU-8	3D	3g
T^3P^2O	6	PKU-10	3D	3m
T^4P^2O	7	$Ge_{10}O_{21}(OH)\cdot N_4C_6H_{21}$	3D	3d
		GeO-JU90	3D	this work

[a]T = tetrahedron, P = trigonal bipyramid, O = octahedron.

compounds, with the only example of the small pore germanate $Ge_{10}O_{21}(OH)\cdot N_4C_6H_{21}$.[3d] In this work, we use the diquaternary ammonium cation 1,5-bis(methylpyrrolidinium)pentane as the structure-directing agent and synthesized a novel open-framework germanate, denoted as GeO-JU90 in a concentrated gel system with H_2O/GeO_2 in a molar ratio of 1.5 in the absence of HF. Its structure is built of 7-connected Ge_7 clusters and additional tetrahedral $GeO_3(OH)$ units, forming a novel interrupted open-framework structure.

As is known, the pore size and channel dimension of a framework structure are crucial factors affecting its application. Those with three-dimensional channels and ring size between 10 and 12 are highly interesting in the catalysis industry. Two of the most famous examples are zeolites beta[9] and ZSM-5[10] in which the former has 12-ring channels and the latter has 10-ring channels. Both of them are important catalysts but with very different catalytic properties due to the very different channel system.[11] Moreover, the recently reported aluminosilicate ITQ-39 has intersecting 10- and 12-ring channels.[12] Because of this unique combination of channels, it shows a very distinct and interesting catalytic property in alkylation of aromatics with olefins. Thus, it is interesting to see more structures combining different sizes of channels. Here, we present GeO-JU90 with a three-dimensional intersecting 12-, 12-, and 11-ring channel system.

Structures of these open-framework materials can be determined routinely by single-crystal X-ray diffraction (SCXRD) if the crystals are big enough. However, in many cases only very fine crystals can be obtained, leaving X-ray powder diffraction (XRPD) and electron crystallography the most promising methods for solving the crystal structure.[13] Due to the sensitivity of germanates under electron beam, electron crystallography could hardly be helpful except for providing unit cell parameters. Therefore, exploring XRPD as a possible technique to reveal the structure for this class of materials is of great importance. Recently, we successfully solved the structure of SU-74 from XRPD data.[14] In this work, the structure of GeO-JU90 was determined from the powder charge-flipping algorithm.[15] It contains 11 independent T atoms, which is one of the most complicated germanates solved from XRPD. Ge K-edge extended X-ray absorption fine structure (EXAFS) analyses were also applied for structural analysis, providing the local atomic structural information around Ge atoms. The guest species in the pores were determined by simulated annealing[16] from XRPD data combining with ^{13}C NMR spectroscopy and other characterization techniques.

EXPERIMENTAL SECTION

Syntheses of SDAs. The SDA for GeO-JU90, 1,5-bis(*N*-methylpyrrolidinium)pentane ($MPP(Br)_2$), was prepared by reacting an excess of *N*-methylpyrrolidine (97%, Aldrich; 20 g, 234.9 mmol) with 1,5-dibromopentane (97%, Aldrich; 18.7 g, 81.3 mmol) in 200 mL of ethanol as a solvent under reflux for 24 h.[17] Then, the solvent was removed by evaporation under vacuum, and the resulting solid was washed with diethyl ether until unreacted amine was completely removed from the solid. The compound was verified by ^1H and ^{13}C NMR. The dibromide salt was converted into the dihydroxide by anion exchange in water solution using an OH^- resin (DOWEX). The extent of exchange was above 90%. The dihydroxide solution was concentrated by rotovaporation under vacuum with mild heating. The final concentration was determined by titration using a certified HCl solution and phenolphthalein. The concentration of $MPP(OH)_2$ is 1.41×10^{-4} mol/g.

The SDA for GeO-ITQ-21, 6-azoniaspiro[5.5]undecane ($C_{12}H_{24}NBr$), was prepared by adding *cis*-2,6-dimethylpiperidine (97%, Aldrich; 10 g, 88.3 mmol) to 1,5-dibromopentane (97%, Aldrich; 20.31 g, 88.3 mmol) in a 1:1 molar ratio in 150 mL of ethanol in the presence of K_2CO_3 (13.41 g, 97.2 mmol) and heated under reflux for 3 days.[18] The product was separated and purified using the above method. The compound was verified by ^1H and ^{13}C NMR. The bromide salt was converted into the hydroxide by anion exchange in water solution using an OH^- resin (DOWEX). The extent of exchange was above 90%. The hydroxide solution was concentrated, and the final concentration was determined by titration using a certified HCl solution and phenolphthalein. The concentration of $C_{12}H_{24}N(OH)$ solution is 2.60×10^{-4} mol/g.

Synthesis of GeO-JU90. Typically, 1.57 g of GeO_2 was dissolved in 26.72 g of $MPP(OH)_2$ solution. The mixture was stirred until a clear solution was obtained. Then the water content was controlled by evaporation of the mixture at 60 °C in an oven. The overall molar ratio of GeO_2:$MPP(OH)_2$:H_2O in the representative synthesis gel was 1.0:0.25:1.5. The final gel was sealed in a Teflon-lined stainless steel autoclave and heated at 150 °C for 15 days. After cooling to room temperature, the white solid was obtained by centrifugation. The product was washed by distilled water and ethanol and dried at room temperature.

Synthesis of GeO-ITQ-21. A 1.05 g amount of GeO_2 was dissolved in 19.20 g of $C_{12}H_{24}N(OH)$ solution. After removing 18.10 g of water by evaporation, 0.25 g of HF (220 μL, 40 wt % in water) was added to the mixture and then stirred by hand. The overall molar composition of GeO_2:$C_{12}H_{24}N(OH)$:HF:H_2O in the gel was 1.0:0.5:0.5:1.5. The final gel was sealed in a Teflon-lined stainless steel autoclave and heated at 150 °C for 15 days. After cooling to room temperature, a white solid of GeO-ITQ-21 was filtered, washed by distilled water and ethanol, and dried at room temperature. GeO-ITQ-21 is isomorphous to silicogermanate zeolite ITQ-21[19] and was used as a standard reference for EXAFS analysis of GeO-JU90.

Structure Solution from Charge Flipping Algorism. XRPD data were collected using a synchrotron X-ray beam with a radiation length of 0.827141 Å at the beamline I11, Diamond Light Source, U.K. Sample was packed in the capillary with a diameter of 0.5 mm, and data were collected from 2° to 60° in 2θ at room temperature with the step size of 0.005°. The pattern was indexed as an orthorhombic unit cell using the indexing program Dicvol04[20] on the first 20 strong peaks (minimum intensity of 5% of the strongest peak). After extraction of

dx.doi.org/10.1021/ic302705f | Inorg. Chem. XXXX, XXX, XXX−XXX

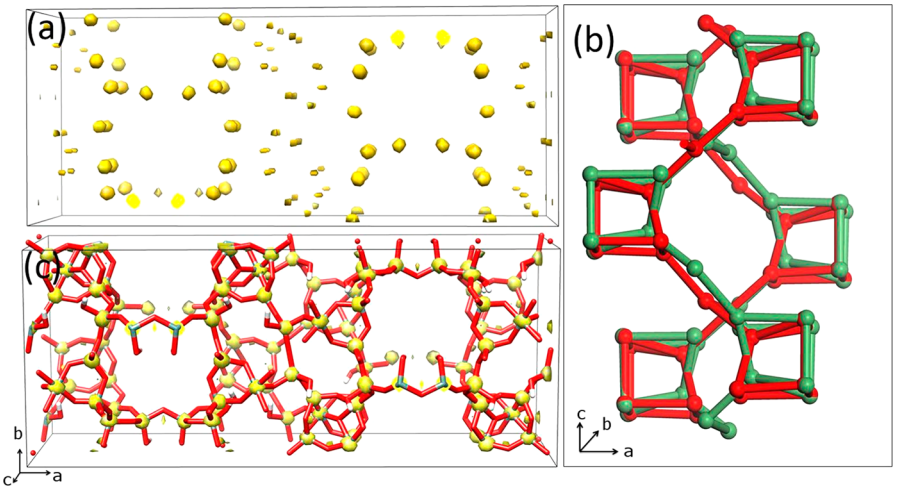

Figure 1. (a) Electron density map obtained from Super Flip with an input space group of *Amam*. (b) Two sets of overlapped Ge_7 clusters in green and red. (c) Final structure model superimposed on the electron density map obtained with an input space group of *Ama*2.

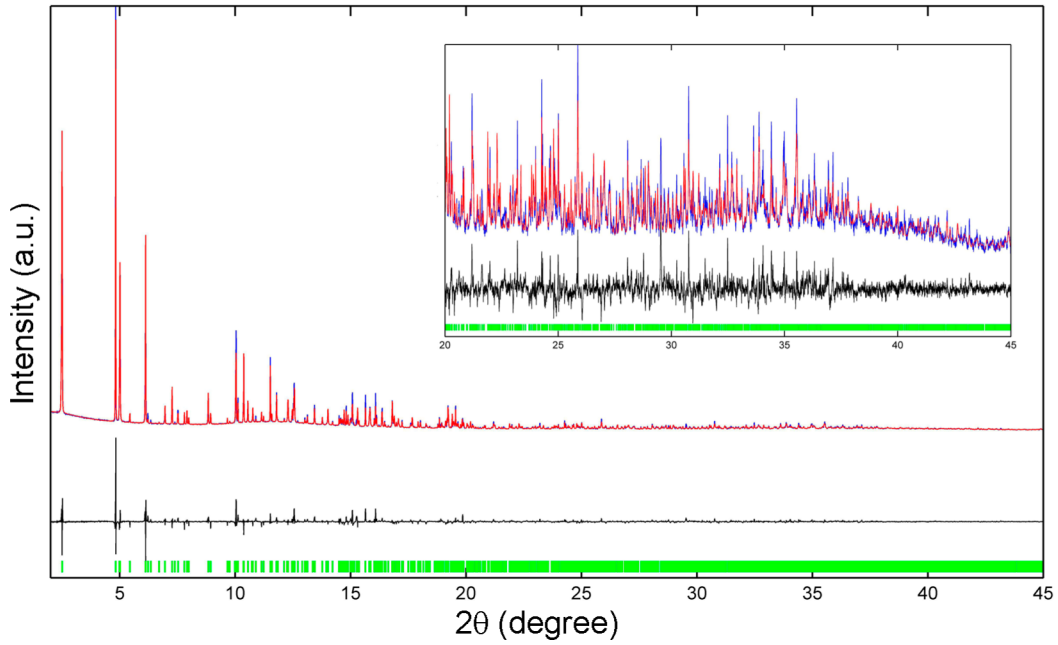

Figure 2. Observed (blue), calculated (red), and difference (black) XRPD patterns for Rietveld refinement of as-synthesized GeO-JU90. (Insert) Patterns in the range from 20° to 45°.

peak intensity with Jana2006,[21] the charge-flipping method was performed using the software Super Flip[22] to solve the structure.

The resulting electron density map in the space group of *Amam* is shown in Figure 1. By assigning the peaks as germanium atoms, the whole framework structure emerges but with disordering in the middle part where peaks are relatively weak. The mirror relating two disordered parts can be removed to convert the space group to *Ama*2, which is also the suggested space group from charge flipping in 4 out of the 10 best results (the other 6 results suggest a space group of *Amam*).

Hence the charge-flipping method was applied again in space group *Ama*2. Then the electron density map was converted to atomic structure using Electron Density Map Analysis (EDMA).[23] All germanium atoms and some of the oxygen atoms could be found directly this time. The remaining oxygen atoms and terminal hydroxyl groups were added to the structure manually based on the coordination geometry. In the asymmetric unit, there are 11 germanium atoms and 27 oxygen atoms, implying the complexity of the structure.

The structure obtained is in space group *Ama*2. However, 56 out of 88 germanium atoms in the structure show the high symmetry of *Amma*, which drove the charge-flipping algorithm to the wrong space group in 6 out of 10 resultant maps. It is also possible that merohedric twinning with 180° rotation along the *a* axis occurs due to the nature of the structure, but different from SC-XRD, twinning does not affect solving the structure from XRPD data.

Structure Refinement of the Framework. Rietveld refinement was applied to all framework atoms using TOPAS[24] with soft restrains on the distance between bonded germanium and oxygen atoms as well as between each pair of oxygen atoms bonded to the same germanium atoms. The topology of GeO-JU90 was determined using the TOPOS package.[25]

Allocation and Refinement of Guest Species. The guest species were found using the simulated annealing method with TOPAS. The first 10 carbon atoms were added to random positions and refined with restrains of minimal distance from framework atoms to prevent clashing. These carbon atoms assembled into groups after running simulated annealing. One was located in the channel along the

dx.doi.org/10.1021/ic302705f | *Inorg. Chem.* XXXX, XXX, XXX−XXX

a axis and had a similar shape as the SDA molecule, while the other two groups of carbon atoms located in the conjunction part of the other two channels perpendicular to the *a* axis could be interpreted as two separated 1-methypyrrolidine molecules, which may imply decomposition of the SDA molecule.

To identify organic species in the channel, solid-state ^{13}C MAS NMR was first carried out on the as-synthesized product. The result was ambiguous, showing three broad peaks. Later, the organic species was extracted after dissolving the framework. As detailed in the following part, the ^{13}C MAS NMR spectrum in the liquid phase proved that the SDA molecules remained intact after the hydrothermal process. This means that the two separated 1-methypyrrolidine molecules were actually connected by a pentane group. However, due to the high flexibility and low electron density of the alkane chain, it was not determined directly from simulated annealing. Therefore, two intact SDA molecules were added as rigid (hydrogen atoms were omitted, and the corresponding number of electrons was assigned to carbon and nitrogen atoms). After refining positions and the configuration of SDA molecules, an additional 8 peaks in the Fourier difference map were found, which could be water or other small cations, e.g., NH_4^+. By considering the charge balance that the framework carries negative charges per unit cell and SDA cations carry 16 positive charges, those peaks were assigned as NH_4^+ ions which came from decomposition of SDA molecules. After overall refinement on both framework and guest species, good fitting was reached as shown in Figure 2 and Table 2.

Table 2. Crystal Data and Refinement Details of Structure Determination of GeO-JU90 from X-ray Powder Diffraction

data collection	
synchrotron facility	Diamond Light Source
beamline	I11
capillary, size	0.5 mm
wavelength	0.827141 Å
2θ range	2–60°
step size	0.005°
refinement	
empirical formula	$\mid(C_{15}N_2H_{32})(NH_4)\mid[Ge_{11}O_{21.5}(OH)_4]$
unit cell formula	$Ge_{88}\ O_{204}\ C_{120}\ N_{24}\ H_{320}$
space group	*Ama*2
a(Å)	37.82959
b(Å)	15.24373
c(Å)	12.83659
unit cell volume	7402.4 Å^3
density	2.637 g/cm^3
2θ range for refinement	2–45°
no. of parameters	188
no. of data points	8601
refinement method	Rietveld refinement
$R_p/R_{wp}/R_{exp}$	6.650%/9.678%/1.859%
R_{brag}	4.781%
GOF	5.205

XAFS Measurement. X-ray absorption fine structure (XAFS) spectra were collected in transmission mode at the Ge K-edge (11.103 KeV) over the energy range 10.900–11.900 KeV at the hard X-ray microanalysis (HXMA) beamline of the Canadian Light Source (Saskatoon, SK, Canada). Powdered samples were measured using a Si (111) monochromator and a rhodium mirror. Samples were packed into a kapton film pouch for measurements. A Ge standard (GeO-ITQ-21) was measured simultaneously with each scan (transmission mode) for the edge energy calibration. XAFS data analysis was performed with the WinXAS 3.1 software package using a similar data reduction procedure as reported elsewhere.[26] Theoretical phase and scattering amplitudes used for fitting experimental data were obtained using the FEFF8.2 computational package.[27] The model used to obtain scattering paths was the crystal structure of GeO_2.[28] Fourier transforms into R space were performed on k^2-weighted EXAFS oscillations in the k range of 2.7–13.0 Å^{-1}, employing Gaussian windows, which was then conducted in R space. All fits performed in the R space include the fitting of the Ge–O distance to the first shell, EXAFS Debye–Waller factor of σ^2 which accounts for thermal vibration (assuming harmonic vibration) and static disorder (assuming a Gaussian pair distribution) at an interatomic Ge–O distance away, the parameter of ΔE_o which accounts for the error in determining the edge energy, and the amplitude reduction factor of S_o^2 which was determined by fitting the standard (GeO-ITQ-21) to give a value of 0.99.

SEM, NMR, IR, Compositional Analyses, TG, and in Situ XRPD. Crystal size and morphology were characterized by scanning electron microscopy (SEM) using a JSM-6700F electron microscope. The as-synthesized product of GeO-JU90 displays the micrometer size of flaky crystals with a diameter of about 1–3 μm (Supporting Information, Figure S1). Liquid-state ^{13}C and ^1H NMR spectra were recorded on a MERCURY "300BB". The solid-state ^{13}C MAS NMR spectrum was recorded on a Bruker AVANCE III 400 WB spectrometer.

The infrared (IR) spectrum was recorded within the 4000–400 cm^{-1} region on a Nicolet Impact 410 FTIR spectrometer using a KBr pellet.

Inductively coupled plasma (ICP) analysis was carried out on a Perkin-Elmer Optima 3300 DV ICP instrument. CHN elemental analysis was carried out with an Perkin-Elemer 2400 elemental analyzer.

Thermogravimetric (TG) analysis was performed on a Perkin-Elmer TGA 7 to study the weight loss associated with decomposition of guest species. The sample was heated from 25 to 800 °C with a heating rate of 10 °C/min in air.

The in situ variable-temperature XRPD data of GeO-JU90 were collected on a Rigaku D/Max-2500 diffractometer with a Cu Kα radiation source (λ = 1.5418 Å), and the heating rate is 10 °C/min from room temperature to 500 °C. Patterns were recorded every 20 °C between 200 and 400 °C. The temperature was equilibrated for 2 min prior to each measurement. The 2θ range was 3–50°.

RESULTS AND DISCUSSION

Structure of GeO-JU90. The structure of GeO-JU90 was determined from synchrotron XRPD data using the charge-flipping algorithm. It reveals that GeO-JU90 crystallizes in the orthorhombic space group of *Ama*2 with lattice parameters a = 37.82959 Å, b = 15.24373 Å, and c = 12.83659 Å. Each asymmetric unit in GeO-JU90 contains 11 crystallographically independent Ge atoms and 27 crystallographically independent O atoms, as shown in Figure 3a. The structure is constructed from Ge_7 clusters and additional tetrahadral $GeO_3(OH)$ units.

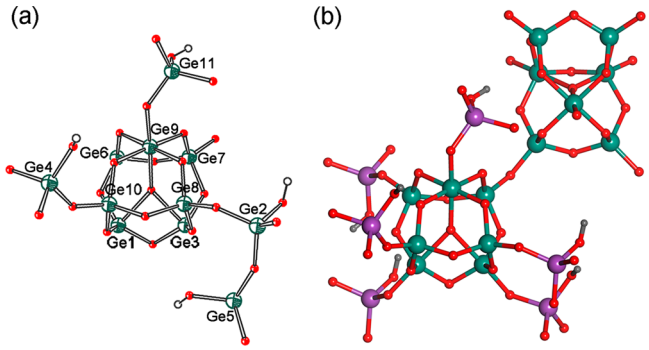

Figure 3. (a) Asymmetric unit of germanate GeO-JU90 (green, Ge; red, O; gray, H). (b) Coordination environment of Ge_7 cluster (green, Ge atoms in Ge_7 cluster; violet, Ge atoms in $GeO_3(OH)$ units; red, O; gray, H).

dx.doi.org/10.1021/ic302705f | Inorg. Chem. XXXX, XXX, XXX–XXX

Figure 3b shows the coordination environment of the Ge_7 cluster. Each Ge_7 cluster connects with seven Ge-centered tetrahedra, of which six are the additional $GeO_3(OH)$ units and one is a GeO_4 tetrahedron that belongs to the adjacent Ge_7 cluster. Such 7-connected Ge_7 cluster has rarely been observed in reported germanates, with the only example of germanate $Ge_{10}O_{21}(OH)N_4C_6H_{21}$ containing 7-ring channels.[3d]

In the structure of GeO-JU90, the Ge_7 cluster can be simplified as a polyhedron with seven vertices corresponding to four GeO_4 tetrahedra, two GeO_5 trigonal bipyramids, and one GeO_6 octahedra as shown in Figure 4a. Each of the two Ge_7

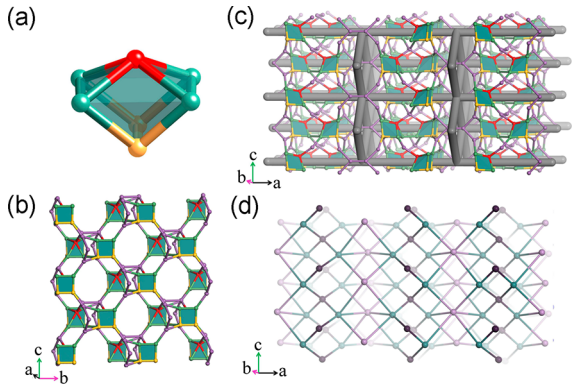

Figure 4. (a) Ge_7 cluster consisting of one GeO_6 octahedron (red), two GeO_5 trigonal bipyramids (yellow), and four GeO_4 tetrahedra (green). (b) Layer built of Ge_7 clusters and extra tetrahedral $GeO_3(OH)$ units (violet). (c) Framework structure with a three-dimensional channel system constructed by assembling the layers. (d) Simplified topological view of the framework, Ge_7 (green), two $GeO_3(OH)$ units (violet), and six $GeO_3(OH)$ units (violet).

clusters is directly connected by corner sharing to form a sort of dimer as shown in Figure 4b. Such dimers are further connected by additional $GeO_3(OH)$ units to build up a layer. The layers possessing 11-ring channels perpendicular to themselves (along the *a* axis) are further assembled via bridging $GeO_3(OH)$ units to form the three-dimensional open-framework germanate. A large pore space consisting of two 12-ring channels perpendicular to the *a* axis is created between two layers. Thus, the framework structure has an interconnected three-dimensional channel system of 11 × 12 × 12-rings (Figure 4c).

To simplify the structure, topology analysis was carried out (Figure 4d and Supporting Information, Table S1). The extra tetrahedral $GeO_3(OH)$ units complicated the connectivity of the Ge_7 cluster. If the Ge_7 cluster was chosen as the uninode, its connectivity could become 17. Thus, we decided to use three different nodes representing Ge_7 clusters (green), two $GeO_3(OH)$ units (violet), and six $GeO_3(OH)$ units (violet). The net obtained has the point symbol of $\{3.4^2.5^2.6\}$-$\{3.4^5.5^3.6^6\}_2\{4^5.5^2.6^8\}$ and transitivity of [3 6 9 5]. After simplification, it is clear that the Ge_7 cluster connects to one of the other Ge_7 clusters directly and connects to as many as 16 clusters though the other nodes.

EXAFS Analysis. Ge K-edge EXAFS analysis was performed to analyze the local structural information around the Ge atoms. The resultant experimental spectrum and best fitting are shown in Figure 5 and Table 3. GeO-ITQ-21 was selected as a standard reference for the edge energy calibration. The fitting result for GeO-ITQ-21 exhibits a first-shell contribution from about 4.0(1) O atoms at an average distance of 1.739(5) Å,

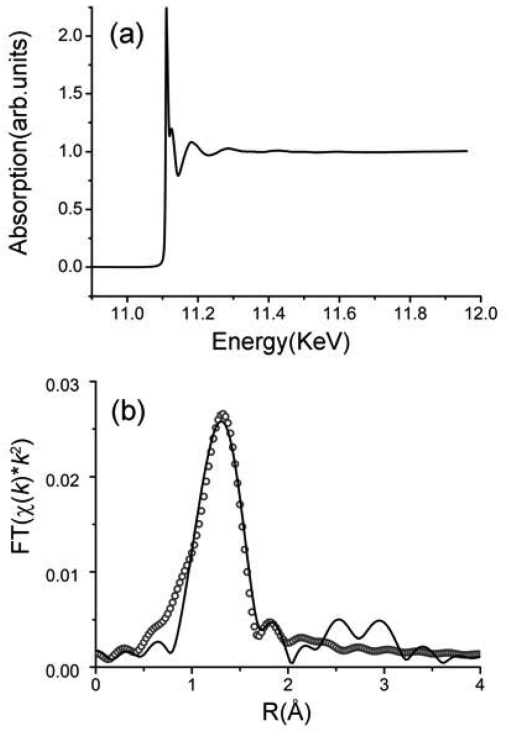

Figure 5. (a) Experimental XAFS data of GeO-JU90 plotted in E space. (b) Experimental FT-EXAFS (solid line) and best fit (open circle) in R space. Fitting was done with a *k* range of 2.7−13.0 $Å^{-1}$.

Table 3. EXAFS Fitting Results for GeO-ITQ-21 and GeO-JU90 with a *k* Range of 2.7−13.0 $Å^{-1}$

sample	R_{Ge-O}(Å)	CN	σ^2 ($Å^2$)	ΔE_o
GeO-ITQ-21	1.739(5)	4.0(1)	0.0027(5)	−1(1)
GeO-JU90	1.750(8)	4.2(2)	0.0048(7)	−4(2)

confirming that only GeO_4 tetrahedra exist in GeO-ITQ-21. However, for GeO-JU90 sample, the first-shell contribution is 4.2(2) from O atoms at an average distance of 1.750(8) Å, suggesting that other Ge-centered polyhedra, such as GeO_5 trigonal bipyramids and GeO_6 octahedra, may coexist with GeO_4 tetrahedra. The result is in agreement with the obtained structure of GeO-JU90 containing one GeO_6, two GeO_5, four GeO_4, and four $GeO_3(OH)$ out of the 11 independent Ge atoms, with an average coordination number (CN) of Ge−O of 4.36 and average Ge−O distance of 1.7693 Å. The Debye−Waller factor σ^2 (evaluation of the ordering of Ge local environment[29]) for GeO-ITQ-21 (0.0027(5) $Å^2$) is smaller than that of GeO-JU90 (0.0048(7) $Å^2$), indicating that the local structure around the Ge atoms in the GeO-JU90 framework is more disordered than that of GeO-ITQ-21.

SDA Molecules in the Channel. The lack of strong interaction between the ogranic species and the framework makes the organic species less ordered in the structure, which introduces difficulty in solving their structure initially. Although from synchrotron XRPD data the organic species was later allocated by real-space method-simulated annealing, it is necessary to confirm the result using other techniques.

Solid-state ^{13}C MAS NMR spectroscopy was used to verify the organic species. Due to the low resolution, only three broad peaks (δ 17.1−27.3, 50.1, and 61.0−67.3) are present in the spectrum (Supporting Information, Figure S2), which can be interpreted as either the SDA molecule or the 1-methylpyr-

dx.doi.org/10.1021/ic302705f | Inorg. Chem. XXXX, XXX, XXX−XXX

odine molecule. Then liquid-state ^{13}C NMR was carried out to get a spectrum with higher resolution. The as-synthesized GeO-JU90 compound was first dissolved in 5 M HF solution to liberate the organic species, and then the solution was neutralized by addition of 2 M sodium hydroxide solution and further extracted with CH_2Cl_2. After evaporating the solvent, the liquid-state ^{13}C NMR measurement was performed on the residual solid dissolved in D_2O (0.5 mL). The resultant ^{13}C NMR spectrum (δ 23.5, 24.5, 25.1, 51.3, 66.1, and 67.5) is identical to that of $MPP(Br)_2$ in D_2O solution (δ 20.6, 23.8, 25.5, 50.7, 66.1, and 66.9) (Supporting Information, Figure S3), suggesting that the MPP^{2+} cations remain intact in the structure of GeO-JU90.

Our structural analysis suggests that part of the SDA molecules decompose to smaller species, i.e., NH_4^+ ions during hydrothermal synthesis. The FTIR spectrum of GeO-JU90 (Supporting Information, Figure S4) shows peaks at around 3000 and 1470 cm^{-1} which can be attributed to NH_4^+ ions.[3d] The absorption bands at 834, 785, and 736 cm^{-1} can be assigned to asymmetric stretching vibrations of Ge−O bonds. The peaks at 581 and 532 cm^{-1} are attributed to the symmetrical stretch of Ge−O bonds. A Ge−O bending vibration is observed at 483 and 454 cm^{-1}.[3d,30]

The number of SDA molecules and NH_4^+ cations in the structure was examined by compositional analyses. ICP analysis gives the contents of Ge as 52.8 wt %, while elemental analyses give the contents of C, H, and N as 12.27, 2.75, and 2.70 wt %, respectively. These compositional analysis results are in agreement with the empirical formula, $|(C_{15}N_2H_{32})(NH_4)|[Ge_{11}O_{21.5}(OH)_4]$, given by the crystal structure determined from XRPD data (calculated value Ge, 54.37; C, 12.26; H, 2.74; N, 2.86 wt %). The fact that the C/N ratio of 5.30 is significantly lower than the C/N ratio of 7.5 for the $MPP(OH)_2$ molecule confirms the presence of NH_4^+ cations as additional counterions decomposed from $MPP(OH)_2$ during hydrothermal synthesis.

The TG curve of GeO-JU90 (Supporting Information, Figure S5) shows a weight loss of 1.9% between 25 and 165 °C, which corresponds to removal of the physically adsorbed water molecules. The weight loss of 20.95% between 165 and 800 °C in the TG curve corresponds to release of NH_3, decomposition of SDA molecules, and loss of OH terminal groups in the form of water molecules (calcd 20.04%). In situ XRPD analysis indicates that the structure collapses at 300 °C with decomposition of SDAs (Supporting Information, Figure S6).

CONCLUSIONS

A novel three-dimensional open-framework germanate GeO-JU90 has been hydrothermally prepared using 1,5-bis-(methylpyrrolidinium)pentane dihydroxide as the structure-directing agent in the concentrated gel system. The framework structure of GeO-JU90 was solved from synchrotron XRPD data using the charge-flipping algorithm. It reveals that the structure contains 11 crystallographically independent Ge atoms and 27 crystallographically independent O atoms, which is one of the most complicated germanate structures. The framework structure is built of 7-connected Ge_7 clusters and additional $GeO_3(OH)$ units forming a three-dimensional interrupted open-framework with intersecting 12 × 12 × 11-ring channels. The Ge K-edge EXAFS analysis provides the local structural information around the Ge atoms in the framework structure. It gives rise to the first-shell contribution from about 4.2(2) O atoms at the average distance of 1.750(8) Å, which is in agreement with the obtained structure. The framework structure consisting of 7-connected Ge_7 clusters and additional $GeO_3(OH)$ units can be described as an assembly of layers with intra 11-ring pores to form a three-dimensional structure with intersecting 12 × 12 × 11-ring channels. The organic species in the channel can be determined by the simulated annealing method and was further confirmed by NMR, IR, compositional analyses, and TG analysis. The SDA molecules could not be removed from the channels while keeping the framework intact. This work not only shows a germanate with a novel structure and interesting channel system but also demonstrates a powerful way for structure solution of complex structures by combing XRPD with the charge-flipping algorithm, simulated annealing, and EXAFS characterization.

ASSOCIATED CONTENT

Supporting Information

SEM images, solid-state ^{13}C MAS NMR spectra, liquid-state ^{13}C NMR spectra, IR spectrum, TG curves, in situ XRPD patterns, and nets that describe the underlying topology of GeO-JU-90. This material is available free of charge via the Internet at http://pubs.acs.org.

AUTHOR INFORMATION

Corresponding Author

*Phone: +86-431-85168608 (J.Y.); +4686747481 (J.S.); 001-902-494 3323 (P.Z.). Fax: +86-431-85168608 (J.Y.); 001-902-494 1310 (P.Z.). E-mail: jihong@jlu.edu.cn (J.Y.); junliang.sun@pku.edu.cn (J.S.); peng.zhang@dal.ca (P.Z.).

Author Contributions

#These authors contributed equally to this work

Author Contributions

This manuscript was written through contributions of all authors. All authors have given approval to the final version of the manuscript.

Notes

The authors declare no competing financial interest.

ACKNOWLEDGMENTS

This project was supported by the National Natural Science Foundation of China and the State Basic Research Project of China (Grant No. 2011CB808703). We also are thankful for support from the Swedish Research Council (VR) and the Swedish Governmental Agency for Innovation Systems (VINNOVA) through the Berzelii Center EXSELENT and the Discovery Grant from NSERC Canada. We thank Beamline I11 in Diamond Light Source, U.K., for XRPD data collection and the Canadian Light Source for XAFS measurements. The Canadian Light Source is financially supported by NSERC Canada, CIHR, NRC, and the University of Saskatchewan. Synchrotron technical support from Yang Xinxin at the Shanghai Synchrotron Radiation Facility and Ning Chen at the Canadian Light Source is also acknowledged.

REFERENCES

(1) (a) Cheetham, A. K.; Férey, G.; Loiseau, T. *Angew. Chem., Int. Ed.* **1999**, *38*, 3268−3292. (b) Davis, M. E. *Nature* **2002**, *417*, 813−821. (c) Wang, Z.; Yu, J.; Xu, R. *Chem. Soc. Rev.* **2012**, *41*, 1729−1741.

(2) (a) Jiang, J.; Yu, J.; Corma, A. *Angew. Chem., Int. Ed.* **2010**, *122*, 3186−3212. (b) Yu, J.; Xu, R. *Acc. Chem. Res.* **2010**, *43*, 1195−1204.

(3) (a) Li, H.; Eddaoudi, M.; Richardson, D. A.; Yaghi, O. M. *J. Am. Chem. Soc.* **1998**, *120*, 8567−8568. (b) Plévert, J.; Gentz, T. M.; Laine, A.; Li, H.; Young, V. G.; Yaghi, O. M.; O'Keeffe, M. *J. Am. Chem. Soc.* **2001**, *123*, 12706−12707. (c) Plévert, J.; Gentz, T. M.; Groy, T. L.; O'Keeffe, M.; Yaghi, O. M. *Chem. Mater.* **2003**, *15*, 714−718. (d) Beitone, L.; Loiseau, T.; Férey, G. *Inorg. Chem.* **2002**, *41*, 3962−3966. (e) Zhang, H.; Zhang, J.; Zheng, S.; Yang, G. *Inorg. Chem.* **2003**, *42*, 6595−6597. (f) Tang, L.; Dadachov, M. S.; Zou, X. *Chem. Mater.* **2005**, *17*, 2530−2536. (g) Christensen, K. E.; Shi, L.; Conradsson, T.; Ren, T.; Dadachov, M. S.; Zou, X. *J. Am. Chem. Soc.* **2006**, *128*, 14238−14239. (h) Shi, L.; Bonneau, C.; Li, Y.; Sun, J.; Yue, H.; Zou, X. *Cryst. Growth Des.* **2008**, *8*, 3695−3699. (i) Guo, B.; Inge, A. K.; Bonneau, C.; Sun, J.; Christensen, K. E.; Yuan, Z.; Zou, X. *Inorg. Chem.* **2011**, *50*, 201−207. (j) Pan, Q.; Li, J.; Christensen, K. E.; Bonneau, C.; Ren, X.; Shi, L.; Sun, J.; Zou, X.; Li, G.; Yu, J.; Xu, R. *Angew. Chem., Int. Ed.* **2008**, *47*, 7868−7871. (k) Pan, Q.; Li, J.; Ren, X.; Wang, Z.; Li, G.; Yu, J.; Xu, R. *Chem. Mater.* **2008**, *20*, 370−372. (l) Ren, X.; Li, Y.; Pan, Q.; Yu, J.; Xu, R.; Xu, Y. *J. Am. Chem. Soc.* **2009**, *131*, 14128−14129. (m) Su, J.; Wang, Y.; Wang, Z.; Liao, F.; Lin, J. *Inorg. Chem.* **2010**, *49*, 9765−9769.

(4) (a) Li, H.; Yaghi, O. M. *J. Am. Chem. Soc.* **1998**, *120*, 10569−10570. (b) Conradsson, T.; Dadachov, M. S.; Zou, X. *Microporous Mesoporous Mater.* **2000**, *41*, 183−191. (c) Medina, M. E.; Iglesias, M.; Monge, M. A.; Gutiérrez-Puebla, E. *Chem. Commun.* **2001**, 2548−2549. (d) Villaescusa, L. A.; Lightfoot, P.; Morris, R. E. *Chem. Commun.* **2002**, 2220−2221. (e) Villaescusa, L. A.; Wheatley, P. S.; Morris, R. E.; Lightfoot, P. *Dalton Trans.* **2004**, 820−824. (f) Xu, Y.; Fan, W.; Chino, N.; Uehara, K.; Hikichi, S.; Mizuno, N.; Ogura, M.; Okubo, T. *Chem. Lett.* **2004**, *33*, 74−75.

(5) (a) Li, H.; Eddaoudi, M.; Yaghi, O. M. *Angew. Chem., Int. Ed.* **1999**, *38*, 653−655. (b) Bu, X.; Feng, P.; Stucky, G. D. *Chem. Mater.* **2000**, *12*, 1505−1507. (c) Sun, K.; Dadachov, M. S.; Conradsson, T.; Zou, X. *Acta Crystallogr., Sect. C* **2000**, *56*, 1092−1094. (d) Zhou, Y.; Zhu, H.; Chen, Z.; Chen, M.; Xu, Y.; Zhang, H.; Zhao, D. *Angew. Chem., Int. Ed.* **2001**, *40*, 2166−2168. (e) Xu, Y.; Fan, W.; Elangovan, S. P.; Ogura, M.; Okubo, T. *Eur. J. Inorg. Chem.* **2004**, 4547−4549. (f) Medina, M. E.; Iglesias, M.; Snejko, N.; Gutiérrez-Puebla, E.; Monge, M. A. *Chem. Mater.* **2004**, *16*, 594−599. (g) Attfield, M. P.; Al-Ebini, Y.; Pritchard, R. G.; Andrews, E. M.; Charlesworth, R. J.; Hung, W.; Masheder, B. J.; Royal, D. S. *Chem. Mater.* **2007**, *19*, 316−322. (h) Ren, T.; Xiao, P.; Xing, X.; Christensen, K. E. *Cryst. Res. Technol.* **2010**, *45*, 1035−1040.

(6) (a) Medina, M. E.; Gutiérrez-Puebla, E.; Monge, M. A.; Snejko, N. *Chem. Commun.* **2004**, 2868−2869. (b) Zou, X.; Conradsson, T.; Klingstedt, M.; Dadachov, M. S.; O'Keeffe, M. *Nature* **2005**, *437*, 716−719. (c) Christensen, K. E.; Bonneau, C.; Gustafsson, M.; Shi, L.; Sun, J.; Grins, J.; Jansson, K.; Sbille, I.; Su, B.; Zou, X. *J. Am. Chem. Soc.* **2008**, *130*, 3758−3759. (d) Inge, A. K.; Peskov, M. V.; Sun, J.; Zou, X. *Cryst. Growth Des.* **2012**, *12*, 369−375. (e) Lorgouilloux, Y.; Paillaud, J.-L.; Caullet, P.; Bats, N. *Solid State Sci.* **2008**, *10*, 12−19. (f) Bonneau, C.; Sun, J.; Sanchez-Smith, R.; Guo, B.; Zhang, D.; Inge, A. K.; Edén, M.; Zou, X. *Inorg. Chem.* **2009**, *48*, 9962−9964.

(7) Lin, Z.; Zhang, J.; Zhao, J.; Zheng, S.; Pan, C.; Wang, G.; Yang, G. *Angew. Chem., Int. Ed.* **2005**, *44*, 6881−6884.

(8) Férey, G. *J. Solid State Chem.* **2000**, *152*, 37−48.

(9) (a) Higgins, J. B.; LaPierre, R. B.; Schlenker, J. L.; Rohrman, A. C.; Wood, J. D.; Kerr, G. T.; Rohrbaugh, W. J. *Zeolites* **1988**, *8*, 446−452. (b) Newsam, J. M.; Treacy, M. M. J.; Koetsier, W. T.; de Gruyter, C. B. *Proc. R. Soc. London* **1988**, *A, 420*, 375−405.

(10) (a) Kokotailo, G. T.; Lawton, S. L.; Olson, D. H.; Meier, W. M. *Nature* **1978**, *272*, 437−438. (b) Olson, D. H.; Kokotailo, G. T.; Lawton, S. L.; Meier, W. M. *J. Phys. Chem.* **1981**, *85*, 2238−2243.

(11) Jae, J.; Tompsett, G. A.; Foster, A. J.; Hammond, K. D.; Auerbach, S. M.; Lobo, R. F.; Huber, G. W. *J. Catal.* **2011**, *279*, 257−268.

(12) Tom, W.; Sun, J.; Wan, W.; Oleynikov, P.; Zhang, D.; Zou, X.; Moliner, M.; Gonzalez, J.; Martínez, C.; Rey, F.; Corma, A. *Nat. Chem.* **2012**, *4*, 188−194.

(13) (a) Sun, J.; Bonneau, C.; Cantín, Á.; Corma, A.; Díaz-Cabañas, M. J.; Moliner, M.; Zhang, D.; Li, M.; Zou, X. *Nature* **2009**, *458*, 1154−1157. (b) Gramm, F.; Baerlocher, C.; McCusker, L. B.; Warrender, S. J.; Wright, P. A.; Han, B.; Hong, S. B.; Liu, Z.; Ohsuna, T.; Terasaki, O. *Nature* **2006**, *444*, 79−81. (c) Xie, D.; Baerlocher, C.; McCusker, L. *J. Appl. Crystallogr.* **2008**, *41*, 1115−1121. (d) Baerlocher, C.; Gramm, F.; Massüger, L.; McCusker, L. B.; He, Z.; Hovmöller, S.; Zou, X. *Science* **2007**, *315*, 1113−1116.

(14) Inge, A. K.; Huang, S.; Chen, H.; Moraga, F.; Sun, J.; Zou, X. *Cryst. Growth Des.* **2012**, *12*, 4853−4860.

(15) Baerlocher, C.; McCusker, L.; Palatinus, L. *Z. Kristallogr.* **2007**, *222*, 47−53.

(16) Kirkpatrick, S.; Gelatt, C. D., Jr.; Vecchi, M. P. *Science* **1983**, *220*, 671−680.

(17) Corma, A.; Chica, A.; Guil, J. M.; Llopis, F. J.; Mabilon, G.; Perdigón-Melón, J. A.; Valencia, S. *J. Catal.* **2000**, *189*, 382−394.

(18) Zones, S. I.; Burton, A. W.; Lee, G. S.; Olmstead, M. M. *J. Am. Chem. Soc.* **2007**, *129*, 9066−9079.

(19) Corma, A.; Díaz-Cabañas, M. J.; Martínez-Triguero, J.; Rey, F.; Rius, J. *Nature* **2002**, *418*, 514−517.

(20) Boultif, A.; Louer, D. *J. Appl. Crystallogr.* **2004**, *37*, 724−731.

(21) Petricek, V.; Dusek, M.; Palatinus, L. *JANA2006, a Crystallographic Computing System*; Institute of Physics, Academy of Sciences of the Czech Republic: Prague, Czech Republic, 2000.

(22) Palatinus, L.; Chapuis, G. *J. Appl. Crystallogr.* **2007**, *40*, 786−790.

(23) van Smaalen, S.; Palatinus, L.; Schneider, M. *Acta Crystallogr.* **2003**, *A59*, 459−469.

(24) Young, R. *The Rietveld Method*; Oxford University Press: Oxford, 1993; pp 1−39.

(25) Blatov, V. *IUCr CompComm Newslett.* **2006**, *7*, 4−38. TOPOS is available at http://www.topos.ssu.samara.ru.

(26) (a) MacDonald, M. A.; Zhang, P.; Qian, H.; Jin, R. *J. Phys. Chem. Lett.* **2010**, *1*, 1821−1825. (b) MacDonald, M. A.; Zhang, P.; Chen, N.; Qian, H.; Jin, R. *J. Phys. Chem. C* **2011**, *115*, 65−69. (c) Padmos, J. D.; Zhang, P. *J. Phys. Chem. C.* **2012**, *116*, 23094−23101.

(27) (a) Ankudinov, A. L.; Ravel, B.; Rehr, J. J.; Conradson, S. D. *Phys. Rev. B* **1998**, *58*, 7565−7576. (b) Simms, G. A.; Padmos, J. D.; Zhang, P. *J. Chem. Phys.* **2009**, *131*, 214703.

(28) Haines, J.; Cambon, O.; Philippot, E.; Chapon, L.; Hull, S. *J. Solid State Chem.* **2002**, *166*, 434−441.

(29) Sevillano, E.; Meuth, H.; Rehr, J. *J. Phys. Rev. B* **1979**, *20*, 4908−4911.

(30) (a) Tarte, P.; Pottier, M. J.; Proces, A. M. *Spectrochim. Acta* **1973**, *29A*, 1017−1027. (b) Paques-Ledent, M. Th. *Spectrochim. Acta* **1976**, *32A*, 383−395. (c) Conradsson, T.; Zou, X. D.; Dadachov, M. S. *Inorg. Chem.* **2000**, *39*, 1716−1720.